JOURNAL OF MATERIALS SCIENCE: MATERIALS IN MEDICINE **16** (2005) 135–142

Characterization of trypsin immobilized on the functionable alkylthiolate self-assembled monolayers: A preliminary application for trypsin digestion chip on protein identification using matrix-assisted laser desorption/ionization time-of-flight mass spectrometry

YU-CHANG TYAN[1,*], JIUNN-DER LIAO[2], SHIANG-BIN JONG[3], PAO-CHI LIAO[1], MING-HUI YANG[4], YIN-WEI CHANG[1], RUTH KLAUSER[5], MICHAEL HIMMELHAUS[6], MICHAEL GRUNZE[6]
[1]Department of Environmental & Occupational Health and [2]Department of Materials Science and Engineering, National Cheng Kung University, No.1, Ta-Hsueh Road, Tainan 701, Taiwan, Republic of China
E-mail: yctyan@mail.ncku.edu.tw
[3]Department of Nuclear Medicine, Kaohsiung Medical University, 100 Shi-Chuan 1st Road, Kaohsiung 807, Taiwan, Republic of China
[4]Department of Chemistry, Texas Christian University, 2800 S. University Drive, Fort Worth, TX 76129, USA
[5]National Synchrotron Radiation Research Center, 101 Hsin-Ann Road, Hsinchu Science Park, Hsinchu 300, Taiwan, Republic of China
[6]Lehrstuhl für Angewandte Physikalische Chemie, Universität Heidelberg, Im Neuenheimer Feld 253, 69120 Heidelberg, Germany

Self-assembled monolayers (SAMs) on coinage metal provide versatile modeling systems for studies of interfacial electron transfer, biological interactions, molecular recognition and other interfacial phenomena. Recently the bonding of enzyme to SAMs of alkanethiols onto Au electrode surfaces was exploited to produce a bio-sensing system. In this work, the attachment of trypsin to a SAMs surface of 11-mercaptoundecanoic acid was achieved using water soluble *N*-ethyl-*N*′-(3-dimethylaminopropyl)carbodiimide hydrochloride and *N*-hydroxysuccinimide as coupling agent. The thickness of SAMs was determined by optical ellipsometer; contact angles of the modified Au surfaces were measured in air using a goniometer. The Second Harmony Generation data displays the last few percents of the alkylthiol molecules adsorbed and produced the complete monolayer by inducing the transition from a high number of gauche defects to an all-*trans* conformation. Using X-ray Photoelectron Spectroscopy (XPS) and Fourier-Transformed Infrared Reflection-Absorption and Attenuated Total Reflection Spectroscopes (FTIR-RAS and ATR), we examined the chemical structures of samples with different treatments. By matrix-assisted laser desorption/ionization time-of-flight mass spectrometry (MALDI-TOF MS), we demonstrated the digestion of bovine serum albumin (BSA) on the trypsin-immobilized SAMs surface.

Experimental results have revealed that the XPS C1s core levels at 286.3 and 286.5 eV (Amine bond), 288.1 eV (Amide bond) and 289.3 eV (Carboxylic acid) illustrate the immobilization of trypsin. These data were also in good agreement with FTIR-ATR spectra for the peaks valued at 1659.4 cm^{-1} (Amide I) and 1546.6 cm^{-1} (Amide II). Using MALDI-TOF MS observations, analytical results have demonstrated the BSA digestion of the immobilized trypsin on the functionalized SAMs surface. For such surfaces, BSA was digested on the trypsin-immobilized SAMs surface, which shows the enzyme digestion ability of the immobilized trypsin. The terminal groups of the SAMs structure can be further functionalized with biomolecules or antibodies to develop surface-base diagnostics, biosensors, or biomaterials.

*Author to whom all correspondence should be addressed.

1. Introduction

Self-assembled monolayers (SAMs) have received a great deal of attention for their fascinating potential technical applications such as nonlinear optics and device patterning [1–3]. They were also used as an ideal model to investigate the effect of intermolecular interactions in the molecular assembly system [4, 5]. It was very convenient to introduce functional structure as tail group on SAMs, and to investigate different molecular interactions with tail group on SAMs as induced by particular species [6, 7].

SAMs form spontaneously by chemisorptions and self-organization of thiolate organic molecules onto a surface of appropriate substrate. SAMs were usually prepared by immersing a substrate into a solution containing a ligand that was reactive to the surface or by exposing the substrate to the vapor of the reactive species.

Nuzzo and Allara utilized dialkyl disulfides formed and oriented monolayers on gold (Au), which shaped a representative series of organic disulfides capable to be absorbed on freshly evaporated Au substrates at room temperature and easily functionalized by disulfide adsorption [8]. Sheen *et al.* reported the discovery of a new class of organized monolayers derived from the self-assembly of alkanethiols directly onto the bare gallium arsenide (GaAs) surface [9]. The preparation of SAMs on single crystal indium phosphide (InP) surfaces was studied indirectly by Lin and Waldeck *et al.* It was found that the alkanethiol compounds might be used to prepare SAMs on the semiconductor InP in a manner, which was quite similar to the use for GaAs [10]. The orthogonal self-assembly of electroactive monolayers on Au and indium tin oxide (ITO) was reported by Gardner *et al*. It showed two systems, which can be used to simultaneously assemble two unique molecular reagents, a thiol with a carboxylic acid and a thiol with a phosphoric acid, as independent monolayers on two different substrates, Au and ITO [11].

Table I lists a number of systems known to give SAMs.

The most characterized system of SAMs was preferably the alkanethiolates (AT) on Au, rather than other metals such as platinum, copper, or silver, because gold did not have a stable oxide. SAMs formed by adsorption of either alkanethiols onto Au or alkylsilanes onto hydroxylated surfaces constitute an important class of model surfaces for fundamental studies of protein or enzyme adsorption. The process was assumed to occur with the loss of hydrogen, by the immersion of Au substrate in a dilute solution of the AT and the formation of well-ordered SAMs on Au surface [8, 12–15]. The AT SAMs not only provide excellent model system to study fundamental aspects of surface properties such as wetting [16] and tribology [17], but also are promising candidates for potential applications in the fields of biosensors [18], biomimetics [19] and corrosion inhibition [20]. Recently the bonding of enzymes to SAMs of AT on Au surfaces has begun to receive attention as a method of constructing enzyme electrodes.

TABLE I Description of SAMs/substrate preparation

Substrate	Ligand or precursor	Expression of binding
Au, Ag, Cu, Pd	RSH, AuSH (thiols)	RS-Au (Ag, Cu, Pd)
GaAs, InP	RSH	RS-GaAs (InP)
Pt	RNC	RNC-Pt
SiO_2, glass	$RSiCl_3$, RSiOR'	Siloxane
Metal oxides	RCOOH, RCONHOH	$RCOO^{-}\ldots MO_n$, $RCONHOH\ldots MO_n$
ZrO_2	RPO_3H_2	$RPO_3^{2-}\ldots Zr^{IV}$
In_2O_3/SnO_2(ITO)	RPO_3H_2	$RPO_3^{2-}\ldots M^{n+}$

In this study, we practice two kinds of the AT SAMs, including: 1-Dodecanethiol and 11-mercaptoundecanoic acid to prepare the SAMs on the Au (111) surface, followed by the coupling of a biological sensing element such as an enzyme, protein, cell or antibody with a transducer, either chemical, electrochemical, optical or piezoelectric, which was regarded as the basis to integrate an enzyme chip. For example, water-soluble *N*-ethyl-*N*′-(3-dimethylaminopropyl)carbodiimide hydrochloride (EDC) and *N*-hydroxysuccinimide (NHS) were utilized to activate the tail group of O═C─OH [21–23] and then immersed in the trypsin-contained solution to bind with $-NH_2$ in trypsin.

As shown in the literatures [24–27], a variety of analytical techniques such as X-ray Photoelectron Spectroscopy (XPS), Infrared Reflection Absorption Spectroscopy (IR-RAS), Fourier-Transformed Infrared with Attenuated Total Reflection (FTIR-ATR), Second Harmonic Generation (SHG), Elliposometer and Contact angle measurements, the AT SAMs were densely packed films. The general understanding was that the molecules were attached to the surface via an Au-thiolate bond, though some results have indicated the possible formation of disulfides. The molecular confirmations of alkyl chains in the completed monolayers were identified by Elliposometer and SHG. The molecular structure and organization of the SAMs were investigated using surface-sensitive techniques such as FTIR-ATR and XPS. A matrix-assisted laser desorption ionization time-of-flight mass spectrometry (MALDI-TOF MS) was used to obtain the fragmentation patterns of tryptic peptides in this study.

In this experiment, it tends to complete a preliminary study for a potential biomedical application of functionalized SAMs to immobilize with enzyme. This type of surface can also be successfully used to develop a feasible procedure of producing surface-base enzyme biochips.

2. Materials and methods

2.1. Formation of SAMs

Au was the most frequently used coinage metal, as it does not have a stable oxide under ambient conditions. A 200 nm thick Au film was prepared by electron beam evaporation onto Si (111) surface (*Silicon Sense*) primed with an adhesion layer of 20 nm Ti. Prior to each experiment, all containers, equipment and supplies were carefully cleaned by first rinsing with absolute ethanol, then with 30% hydrogen peroxide, again with absolute ethanol, and finally with the pure solvent to be used in the adsorption experiments. The Au (111) substrates with a standard dimension of 1.5 × 1.5 cm were

cleaned by H_2O_2 solution for 15 sec followed rinsing by high-purity ethanol (RDH 32205, Riedel-deHaën), and then immersed into 0.5 mM ethanolic alkanethiol solution at room temperature for 12 hrs [24, 27]. The alkanethiols adsorb spontaneously from solution onto the Au surface. Two kinds of chemicals for SAMs preparation were used: 1-Dodecanethiol: $C_{12}H_{26}S$ (44130, Fluka), and 11-mercaptoundecanoic acid: $C_{11}H_{22}O_2S$ (450561, Aldrich). The reference surface for IR-RAS: $C_{20}D_{42}S$ was utilized. The functionalized thiol groups were chemisorbed onto Au surface via the formation of thiolate bonds [28].

2.2. Immobilisation of trypsin onto SAMs

To immobilize trypsin, the 11-mercaptoundecanoic acid/Au surface was immersed in the coupling agent: 75 mM, *N*-ethyl-*N*′-(3-dimethylaminopropyl) carbodiimide hydrochloride (EDC, E-6383, Sigma) and 15 mM, *N*-hydroxysuccinimide (NHS, H-7377, Sigma) at 4 °C for 30 min [25, 29, 30]. Water-soluble EDC and NHS were used for activating O═C─OH [22, 23] and then the EDC-NHS buffer was removed and replaced by the 0.2 μg/μl (w/v) trypsin digestion buffer (V511A, Promega) at 4 °C for 24 hrs. The SAMs wafer was thereafter washed by DI water and dried out mildly at 4 °C. The preparation was carried out in a clean environment. During the reactions, EDC was capable to convert the carboxylic acids into a reactive intermediate, which was susceptible to be attacked by amine group. In some cases, both of EDC and NHS were used as they produce a more stable reactive intermediary, which has been shown to give a greater reaction yield [18].

2.3. Ellipsometric measurement

The thickness of the SAMs monolayers was determined by an optical ellipsometer (LPS-400, J. A. Woollam Co., Inc.), equipped with a He/Ne laser of $\lambda = 632.8$ nm as the light source. The light has an incident angle of 70 °, relative to the surface normal. After monolayer formation, each sample was analyzed, and the film thickness was calculated from three-phase parallel layer model: ambient, organic film, and Au substrate models. Using the average complex refractive index of the individual sample and a real refractive index of 1.45 for the film. The value of 1.45 was representative for the adsorbate precursors, which facilitated a comparison with the thickness that has been reported for a variety of monolayers elsewhere [26, 31].

2.4. Contact angle measurement

The contact angles (θ) were measured in air using a goniometer (Krüss apparatus). A Milli-Q grade water (Millipore Co., Inc.) was used to contact with the sampling dimension by the sessile drop method. For this measurement, a 2 μl droplet was placed slightly on the specimen with the needle of a syringe. The value of θ was determined as the volume of the droplet was slowly increased [26, 31].

2.5. X-ray Photoelectron spectroscopy measurement

XPS spectra were acquired with a Physical Electronics PHI 1600 ESCA photoelectron spectrometer with a magnesium anode at 400 W and 15 kV–27 mA (Mg K_α 1253.6 eV, type 10-360 spherical capacitor analyzer). The specimens were analyzed at an electron take-off angle of 70°, measured with respect to the surface plane. The operating conditions were as follows: pass energy 23.4 eV, base pressure in the chamber below 2×10^{-8} Pa, step size 0.05, total scan number 20, scan range 10 eV (for multiplex scan). The peaks were quantified from high-resolution spectra, obtained by using a monochromatic Mg X-ray source. Elemental compositions at the surface using C 1s, O 1s and N 1s core level spectra were measured and calculated from XPS peak area with correction algorithms for atomic sensitivity. The XPS spectra were fitted using Voigt peak profiles and a Shirley background.

2.6. Second harmonic generation measurement

A Nd:Yag laser with a fundamental wavelength of $\lambda = 1064$ nm, a pulse duration of 40 ps, and a repetition rate of 10 Hz was applied. The impinging beam onto the surface had a diameter of around 2.5 mm, and the energy of the laser pulses incident on the samples was about 200 μJ. The light intensity remains far below the damage threshold of the surface. A color filter was placed between the polarizer and the sample to block unwanted fluorescence and second harmonic generation background from the optics. The frequency-doubled light of $\lambda = 532$ nm generated in reflection on the Au surface passed a filter to block the fundamental radiation, a polarized, and a monochromator with a photomultiplier. For each data point, the signals of 20 laser shots were averaged, yielding a temporal resolution of 2 s. The energy of each laser pulse was measured with a pyroelectric detector, the output of which served to normalize the SHG signal of the sample. In all experiments both the incident fundamental and analyzed second harmonic beam were polarized parallel to the plane of incidence.

In this study, ethanol was used as solvent, and two kinds of molecules for the preparation of SAMs surfaces were studied: 1-Dodecanethiol and 11-mercaptoundecanoic acid. Since the thiol concentrations were in the millimolar region, all solutions of the ethanolic alkanethiol had the same concentration of 0.5 mM [24, 27]. The adsorption experiments were performed in a home-built liquid cell consisting of a Teflon cell and a Suprasil window sealed with an indium wire. The cell had a volume of about 500 μl and was connected to reservoirs. The laser radiation was incident at an angle of 45° with respect to the surface of the cover glass. At the beginning of each experiment, the sample cell was filled with pure solvent to obtain a reference value for the signal intensity and further to check on stability of the signal. After 10 min, the pure solvent was exchanged by the respective solutions.

2.7. Fourier-transformed infrared reflection-absorption and attenuated total reflection spectrosocopies

All infrared (IR) spectroscopy optical benches were acquired with a conventional Fourier-transformed (FT) Spectrometer (FTS-175C, Bio-Rad) equipped with a KBr beam splitter and a high-temperature ceramic source. Win-IR, Win-IR Pro (Bio-Rad) and Origin 6.0 (Microcal Software, Inc.) were used for the data acquisition and analysis. The IR spectra were obtained using p-polarized beam incident at a grazing angle of around 80° with respect to the surface normal. The spectra were measured by a liquid-nitrogen cooled, narrow band MCT detector. The spectra were recorded with a resolution of 4 cm^{-1} using about 500 scans and an optical modulation of 15 kHz filter. Alternatively, the analytical instruments for identifying chemical structures (Amide I and Amide II) was confirmed by FTIR spectrometry, using a Jasco-410 FTIR spectrometer fitted with an Attenuated Total Reflection (ATR, Pike Instrument) device containing a germanium crystal and Harrick KBr prism with 200 scans and spatial resolution of 2 cm^{-1}.

2.8. MALDI-TOF MS instrumentation

The MALDI-TOF MS spectra were acquired on a Voyager DE-PRO Biospectrometry Workstation (Applied Biosystems) in the reflector mode using a nitrogen laser (VSL-337, 337 nm). Mass spectra were collected in the positive-ion mode using an acceleration voltage of 25 kV and a delay of 300 ns. The grid voltage, guide wire voltage, and low mass gate were set to 90.0%, 0.15%, and 3000.0 m/z, respectively. Each mass spectrum collected represents the sum of the data from 100 laser shots.

2.9. MALDI-TOF MS sample preparation

The bovine serum albumin (BSA, 100 femto-mole (fmol), A3311, Sigma) was prepared for MALDI analysis using a conventional dried droplet protocol in which α-cyano-4-hydroxycinnamic acid (CHCA, 55272, Fluka) was used as the matrix. The CHCA matrix was prepared as a saturated, aqueous solution that contains 50% (v/v) acetonitrile and 0.1% (v/v) trifluoroacetic acid (TFA).

In the direct MALDI-TOF MS analysis of BSA, 2 μl of the pooled BSA sample described above was deposited on the trypsin-immobilization surface. The sample was allowed to shake slowly at 37 °C, 30 min using a incubator for digestion and then added 10 μl of CHCA matrix to air-dry at room temperature. Generally, two MALDI-TOF mass spectra were collected at different positions within the same crystallized sample spot.

2.10. Mass spectral analysis

The data in each mass spectrum were visualized using the software (Data Explorer V 4.0; Applied Biosystems) provided by the manufacturer. The resulting peptide mass fingerprints were compared to databases using the program MS-Fit, available at the World Wide Web site at the University of California at San Francisco (http://prospector.ucsf.edu/).

3. Result and discussion

3.1. Surface characterization: film thickness and contact angles

An important metric for the quality of a SAMs surface was given by a direct measurement of the mass coverage of the adsorbate on the surface. Ellipsometry was an invaluable technique for measuring the thickness of alkanethiols adsorbed on SAMs surface, and it was also a useful method to provide key insights into the surfaces of SAMs formed on a variety of metal substrates (e.g., Au, Ag, and Al) [32]. Analytical result from ellipsometry and contact angle measurements of SAMs were summarized in Table II. The optical ellipsometric characterization obtains a film thickness of 16.57 ± 0.55 Å for 11-mercaptoundecanoic acid/Au, and 14.67 ± 0.46 Å for 1-Dodecanethiol/Au, consistent with the formation of films of one molecular layer. The thickness coincides well with what has been reported previously [26, 27, 31]. The ellipsometric measurement yields SAMs thickness close to an expected value from space-filling models with a chain-tilt of approximately 30° from the surface normal.

Contact angles for 1-Dodecanethiol/Au surface was indicative of a well-ordered and homogeneous layer with methyl group at the monolayers/ambient interface. Measurement of 11-mercaptoundecanoic acid/Au using water as probe liquid give advancing contact angles of less than 15°, consistent as a high free energy surface. The SAMs surfaces with the carboxylate or hydroxyl tail group were therefore polarizable and hydrophilic [33]. The contact angles agreed well with Smith *et al.* [26], Lestelius *et al.* [31] and Laibinis *et al.* [34]. The above measurements were found unaffected by extending immersion time in the thiol-containing solutions.

3.2. Investigation of film structure by FTIR-RAS

All monolayer assemblies were routinely characterized with FTIR-RAS upon preparation. Fig. 1 shows that the FTIR-RAS spectra of the SAMs of the alkane and carboxylic acid. The position of the C—H stretching bands of the methylene groups of the alkyl chains indicates the order of the alkyl chains within SAMs. In the spectrum of the SAMs, two absorption bands

TABLE II Ellipsometric thickness and water contact angles measurement of the SAMs on Au (111)

Monolayer compound		Thickness (Å)	Contact angle (deg)
SD-$(CD_2)_{19}$-CD_3	(for IR reference)	25.68 ± 0.60	105.17 ± 0.42
SH-$(CH_2)_{11}$-CH_3	1-Dodecanethiol	14.42 ± 0.55	97.00 ± 0.29
SH-$(CH_2)_{10}$-COOH	11-mercaptoundecanoic acid	16.57 ± 0.55	14.67 ± 0.46

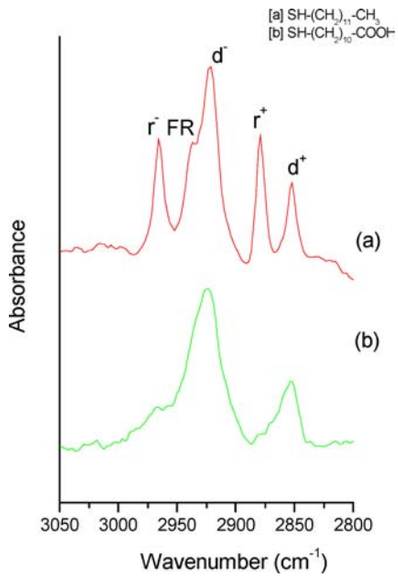

Figure 1 FTIR-RAS spectra show the high-frequency region: 3050–2800 cm^{-1} of the SAMs (a) 1-Dodecanethiol, (b) 11-mercaptoundecanoic acid.

at 2918 and 2850 cm^{-1} were assigned to asymmetric (d^-) and symmetric (d^+) C─H stretching bands of the methylene groups, respectively [34]. The peak positions of CH_3 stretching modes were consistent with the presence of a dense crystalline-like phase: r^+, 2876 cm^{-1}; FR, 2935 cm^{-1}; r^-, 2963 cm^{-1} (Table III). These represent in good agreement with Laibinis *et al.* [34] and Lestelius *et al.* [31], who have identified the peaks as the presence of alkene species. The band positions of 11-mercaptoundecanoic acid/Au given in Table III indicate that the band frequencies at 1705 cm^{-1} and 1400 cm^{-1} were assigned to residual carboxylic acid stretch, ν(C═O) and symmetric carboxylate stretch, $\nu_s(COO^-)$, respectively [25].

3.3. Analysis of SHG data

The second harmonic signal from an adsorbate/substrate system was proportional to the absolute square of the total nonlinear susceptibility $\chi_{tot,}$ which can be described as [24]

$$\chi_{tot} = \chi_{sub} + \chi_{int}(\theta(t)) + \chi_{ads}(\theta(t)) \qquad (1)$$

TABLE III Observed peak position and assignments for the different monolayers

1-Dodecanethiol $SH\text{-}(CH_2)_{11}\text{-}CH_3$	11-Mercaptoundecanoic acid $SH\text{-}(CH_2)_{10}\text{-}COOH$	Assignment [27, 33, 35]
2963		$\nu_{as}(CH_3)$, r^-
2935		$\nu_s(CH_3)$, FR
2918	2918	$\nu_{as}(CH_2)$, d^-
2876		$\nu_s(CH_3)$, r^+
2849	2850	$\nu_s(CH_2)$, d^+
	1705	ν(C═O)
	1400	$\nu_s(COO^-)$

$\nu_{s/as}$: Symmetric/asymmetric-stretching modes. FR: Fermi resonance.

The subscripts denote the contributions originating from the substrate χ_{sub}, the adsorbate χ_{ads}, and their mutual interaction χ_{int}, and $\theta(t)$ was the time-dependent coverage. In our case, Equation (1) simplifies to a superposition of the substrate and the interaction term. As verified experimentally, χ_{ads} can be neglected in the case of alkanethiols due to the low hyperpolarizability of C─H bounds at a fundamental wavelength of 1064 nm.

SHG was applied to check on final coverage as obtained by the various molecules under study. As coverage and SHG intensity were linked by the relation as follow [24],

$$\theta(t) \propto 1 - \sqrt{I_{SHG}(t)} \qquad (2)$$

final coverage of different molecules can be compared by

$$\frac{\theta_1(\infty)}{\theta_2(\infty)} \propto \frac{1 - \sqrt{I_{SHG,1}(\infty)}}{1 - \sqrt{I_{SHG,2}(\infty)}} \qquad (3)$$

Fig. 2 displays the SHG-data thus obtained. All the various molecules induce basically the same drop in intensity, i.e. yield a similar final coverage according to Equation (3). Interestingly, the drop in intensity was slightly larger for the carboxyl-terminated SAM. Possibly, this was due to partial deprotonation of the carboxyl groups, which might affect the electron system of Au.

3.4. Structural confirmation of trypsin-immobilized surfaces

In this experiment, water-soluble carbodiimide EDC and NHS are used to convert the carboxylic acid of the 11-mercaptoundecanoic monolayer to NHS ester. Reaction of this activated the 11-mercaptoundecanoic-NHS ester monolayer with an aqueous solution of an amine or either ammonia, creates an amide bond with the surface. In Fig. 3, the peak at 1407.2 cm^{-1} was usually assigned to carboxylata stretch (COO^-). The peak at 1659.4 cm^{-1} was usually assigned to Amide I (R-CONHR', C═O stretching) and the peak

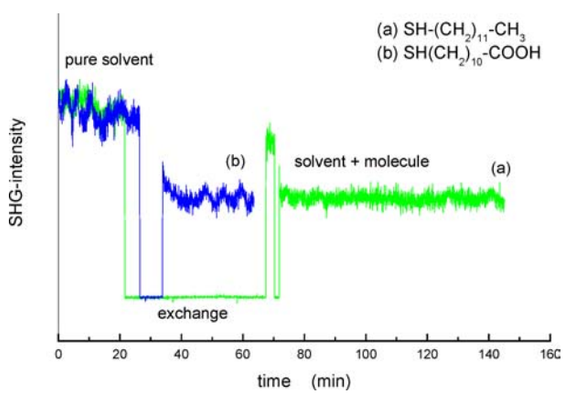

Figure 2 SHG experiments on functionalized thiols of the SAMs, (a) 1-Dodecanethiol, (b) 11-mercaptoundecanoic acid.

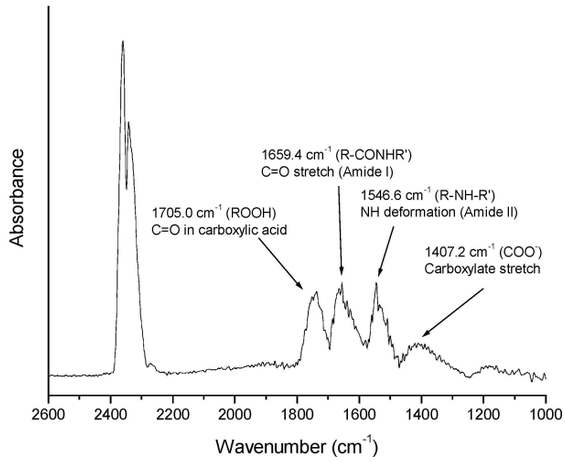

Figure 3 FTIR spectra of the modified SAMs surface: trypsin immobilized on the 11-mercaptoundecanoic acid SAMs surface.

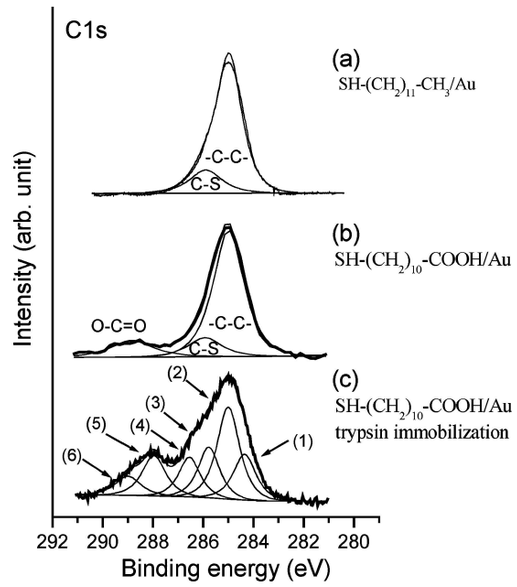

Figure 4 XPS C 1s core level spectra of the modified SAMs surface, (a) 1-Dodecanethiol, (b) 11-mercaptoundecanoic acid, and (c) 11-mercaptoundecanoic acid with trypsin immobilized.

at 1546.6 cm^{-1} to Amide II (R-NHR', NH deformation, N-H bending and C—N stretching). These are in good agreement with Ito *et al.* [35], Kang *et al.* [22] and Tyan *et al.* [23, 36], who have identified the peaks as the presence of O=C—NH species, derived from carboxylic acid and trypsin, where the O=C—OH bond was activated to form O=C—O· by adding water soluble EDC. Thus, the poly-complex between trypsin and 11-mercaptoundecanoic acid was formed; amino groups in trypsin form complexes with carboxyl groups in 11-mercaptoundecanoic acid. Typical chemical compositions of the immobilized trypsin were furthermore characterized using surface sensitive XPS measurement (Fig. 4).

Surface analyses used XPS to measure the binding structure on the SAMs metal surface. The binding energy of C1s core level at 289.3 eV (O=C—O) (Fig. 4(b)) and of O 1s core level at 532.0 eV and 533.3 eV examined by XPS, could be assigned to the O=C—O structure, which was the characteristic group of 11-mercaptoundecanoic acid.

The XPS C1s core level spectra for the trypsin-immobilized SAMs were shown in Fig. 4(c). The curves were fitted in accordance with references 37 and 38. The spectrum was deconvoluted into six peaks: 284.6 and 285.4 eV (hydrocarbon and carbon), 286.3 and 286.5 eV (C with N, amine), 288.1 eV (C with O, carbonyl or amide bond), and 289.3 eV (C with O, carboxylic acid), respectively [37, 38]. The trypsin-immobilized SAMs surface displayed a significant increase of C—N and amide group. The groups were corresponding with trypsin molecules (C—N) or a complex between trypsin and 11-mercaptoundecanoic acid (amide group). In Fig. 4(c), the binding energy at 286.3 and 286.5 eV was assigned to C—N binding in trypsin. The O=C—OH group altered notably owing to the participation of functional group of the 11-mercaptoundecanoic acid binding with trypsin as amide group.

In the XPS measurements, the variations of O1s and N1s with respect to C1s signal ratios are correlated with the significant presence of chemical on the trypsin-immobilized SAMs surface, respectively.

TABLE IV Peptide mass fingerprint of the trypsin digest of BSA with the corresponding database search result using MS-Fit. MS-Fit search selects 9245 entries (results displayed for top 5 matches)

	MOWSE score	#/17(%) Masses matched	% Cov	% TIC	Mean Err Da	Data Tol Da	MS-Digest Index #	Protein MW (Da)/pI	Accession #	Species	Protein name
1	1491	12 (70)	24.5	70.6	0.122	0.782	1076688	69294/5.8	1351907 M	BOVIN	Serum albumin precursor (Allergen Bos d 6)
2	1490	12 (70)	24.0	70.6	0.122	0.782	351651	69324/5.8	30794280 M	UNREADABLE	gi|30794280|ref|NP_851335.1| albumin [Bos taurus]
3	561	10 (58)	22.0	58.8	0.108	0.846	795435	69271/5.8	418694	BOVINE	Serum albumin precursor [validated]
4	507	9 (52)	11.0	52.9	−0.103	0.992	425759	93105/9.2	28565277 M	UNREADABLE	gi|28565277|ref|NP_787948.1| protein Phosphatase I; HLA-C adjacent transcript 53 [Mus musculus]
5	468	5 (29)	17.0	29.4	−0.188	0.966	765083	30635/4.9	15341784	MUS MUSCULUS	Eef1d protein

TABLE V Peptide mass fingerprint of the trypsin digest of BSA. Result of the database search using MS-Fit. BSA was identified with a peptides cover 24.5% (149/607AA's) and a sequence coverage of 70.6% (12/17)

m/z Submitted	MH^+ Matched	Delta Da	Modifications	Start	End	Missed cleavages	Database sequence
927.70	927.49	0.21		161	167	0	(K) YLYEIAR (R)
974.62	974.46	0.16		37	44	0	(K) DLGEEHFK (G)
1163.88	1163.63	0.25		66	75	0	(K) LVNELTEFAK (T)
1249.88	1249.62	0.26		35	44	1	(R) FKDLGEEHFK (G)
1307.01	1306.69	0.32		402	412	0	(K) HLVDEPQNLIK (Q)
1440.16	1439.81	0.35		360	371	1	(R) RHPEYAVSVLLR (L)
1479.01	1478.79	0.22		221	232	2	(R) LRCASIQKFGER (A)
1479.01	1479.80	−0.79		421	433	0	(K) LGEYGFQNALIVR (Y)
1480.13	1479.80	0.33		421	433	0	(K) LGEYGFQNALIVR (Y)
1568.13	1567.74	0.39		347	359	0	(K) DAFLGSFLYEYSR (R)
1568.13	1568.67	−0.54		387	399	0	(K) DDPHACYSTVFDK (L)
1641.36	1640.98	0.38		437	451	1	(R) KVPQVSTPTLVEVSR (S)
2046.51	2045.98	0.53		168	183	1	(R) RHPYFYAPELLYYANK (Y)
2048.52	2048.87	−0.35	1Met-ox	101	117	1	(K)VASLRETYGDMADCCEK(Q)

Acc. #:1351907; Species: BOVIN; Name: Serum albumin precursor; (Allergen Bos d 6)
Index: 1076688; MW: 69294 Da; pI: 5.8

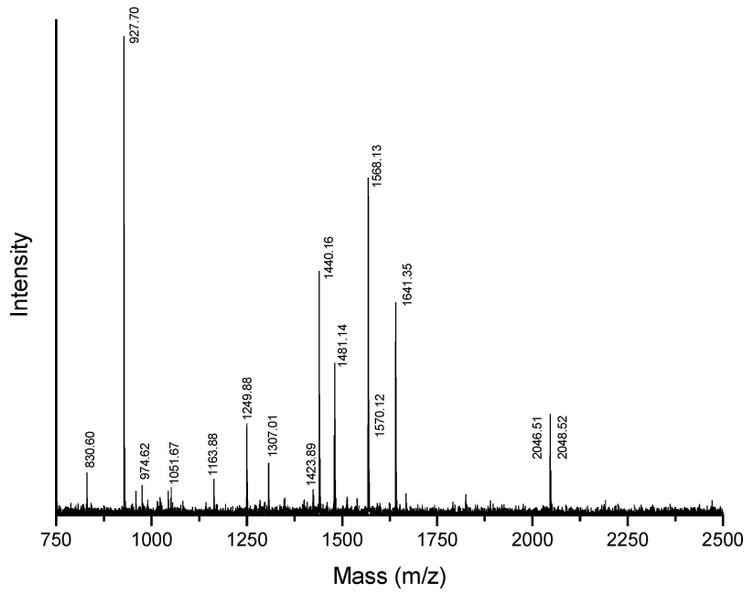

Figure 5 MALDI-TOF MS spectrum of the BSA sample. The result of peptide mass fingerprint of the trypsin digest of BSA using Data Explorer.

3.5. Protein digestion and identification

The purpose of this work is to develop an on-line immobilized trypsin digestion chip for handing minute protein samples at low concentrations and small volumes. The analysis of BSA sample that have been digested by trypsin means can be performed using MALDI-TOF MS for determination of the protein identification. The database search with MS-Fit was performed using the recorded peptide mass fingerprint data sets. Table IV and Fig. 5 showed the MALDI-TOF MS result and spectrum of BSA. In this experiment, 2 μl BSA solution deposited and digested on the trypsin-immobilization surface was analyzed. The MS-Fit search of the data yielded BSA as the top hit with a MOWSE score of 1491, and the sequence coverage of 24%, corresponding to 12 peptide matches (Table V). This result demonstrated that 2 μl of a 100 fmol BSA was sufficient for protein identification. The ability to rapidly and efficiently digest and identify an unknown protein or interest would be of great utility in diagnosing or investigating disease on a proteome-wide scale. Limitations for peptide mass mapping analysis consist of manual sample manipulation steps and extended reaction times for proteolytic digestion. The resultant trypsin digests can be directly analyzed using MALDI-TOF MS, or further concentrated and resolved using chromatographic and electrophoretic separations prior to the mass spectrometry analysis. Such enhancement is particularly attractive for the analysis of complex protein mixtures with a significant difference in their individual concentrations

4. Conclusion

The results presented provide an example of the 11-mercaptoundecanoic acid SAMs applications for the enzyme digestion chip. SAMs formation provides an easy way to prepare the structure that can be further functionalized with biomolecules to yield biorecognition surfaces for use in medical devices. The carboxyl functional thiol monolayer gives an excellent way to

immobilize enzyme, protein or other biomolecules for selective sensing of different analyte. The application of SAMs for the immobilization of enzymes to Au surfaces has considerable potential to produce reproducible enzyme biochips. In summary, we have presented the modification of Au interface via 11-mercaptoundecanoic acid SAMs and proved that the SAMs on Au can be a trypsin digestion chip for protein analysis by MALDI-TOF MS. The materials of SAMs are easy to be obtained, and this method is simple and easy to develop surface-base diagnostics, biosensors, or biomaterials.

Acknowledgment

The authors would like to thank National Science Council (NSC92-2113-M006-022, NSC92-2811-M006-009) and National Health Research Institutes (NHRI 92A1-NSCLC-21-5) Taiwan, R.O.C. for providing research grants.

References

1. J. C. HORNE and G. J. BLANCHARD, *J. Am. Chem. Soc.* **120** (1998) 6336.
2. F. MORHARD, J. SCHUMACHER, A. LENENBACH, T. WILHELM, R. DAHINT, M. GRUNZE and D. S. EVERHART, *Proc. - Electrochem. Soc.* **97**(19) (1997) 1058.
3. K. BIERBAUM, M. GRUNZE, A. BASKI, L. F. CHI, W. SCHREPP and H. FUCHS, *Langmuir* **11** (1995) 2143.
4. A. SCHERTEL, C. WOLL and M. GRUNZE, *J. Phys. IV.* **7** (1997) 537.
5. C. YAN, M. ZHARNIKOV, A. GOELZHAEUSER and M. GRUNZE, *Langmuir* **16** (2000) 6208.
6. H. J. HIMMEL, K. WEISS, B. JAEGER, O. DANNENBERGER, M. GRUNZE and C. WOELL, *ibid.* **13** (1997) 4943.
7. C. JUNG, O. DANNENBERGER, Y. XU, M. BUCK and M. GRUNZE, *ibid.* **14** (1998) 1103.
8. R. G. NUZZO and D. L. ALLARA, *J. Am. Chem. Soc.* **105** (1983) 4481.
9. C. W. SHEEN, J. X. SHI, J. MARTENSSON, A. N. PARIKH and D. L. ALLARA, *ibid.* **114** (1992) 1514.
10. Y. GU, Z. LIN, R. A. BUTERA, V. S. SMENTKOWSKI and D. H. WALDECK, *Langmuir* **11** (1995) 1849.
11. T. J. GARDNER, C. D. FRISBIE and M. S. WRIGHTON, *J. Am. Chem. Soc.* **117** (1995) 6927.
12. C. D. BAIN, E. B. TROUGHTON, Y. TAO, J. EVALL, G. M. WHITESIDES and R. G. NUZZO, *ibid.* **111** (1989) 321.
13. A. ULMAN, in "An Introduction to Ultrathin Origanic Films" (Academic Press, San Diego, 1991).
14. L. H. DUBOIS and R. G. NUZZO, *Annu. Rev. Phy. Chem.* **43** (1992) 437.
15. A. ULMAN, *Chem. Rev.* **96** (1996) 1533.
16. P. E. LAIBINIS, R. G. NUZZO and G. M. WHITESIDES, *J. Phys. Chem.* **96** (1992) 5097.
17. S. A. JOYCE, R. C. THOMAS, J. E. HOUSTON, T. A. MICHALSKE and R. M. CROOKS, *Phys. Rev. Lett.* **68** (1992) 2790.
18. J. J. GOODING and D. B. HIBBERT, *Trends in Analytical Chemistry* **18** (1999) 525.
19. C. ERDELEN, L. HÄUSSLING, R. NAUMANN, H. RINGSDORF, H. WOLF, J. YANG, M. LILEY, J. SPINKE and W. KNOLL, *Langmuir* **10** (1994) 1246.
20. P. E. LAIBINIS and G. M. WHITESIDES, *J. Am. Chem. Soc.* **114** (1992) 9022.
21. D. G. BUERK, in "Biosensor: Theory and Applications" (Tech. Pub. Comp. Inc, 1993).
22. I. K. KANG, B. K. KWON, J. H. LEE and H. B. LEE, *Biomaterials* **14** (1993) 787.
23. Y. C. TYAN, J. D. LIAO, R. KLAUSER, I. D. WU and C. C. WENG, *ibid.* **23** (2002) 65.
24. O. DANNENBERGER, M. BUCK and M. GRUNZE, *J. Phys. Chem. B.* **103** (1999) 2202.
25. B. L. FREY and R. M. CORN, *Anal. Chem.* **l 68** (1996) 3187.
26. E. L. SMITH, C. A. ALVES, J. W. ANDEREGG, M. D. PORTER and L. M. SIPERKO, *Langmuir* **8** (1992) 2707.
27. L. SUN, R. M. CROOKS and A. J. RICCO, *ibid.* **9** (1993) 1775.
28. Y. MIURA, S. KIMURA, Y. IMANISHI and J. UMEMURA, *ibid.* **15** (1999) 1155.
29. C. J. DELDEN, J. P. LENS, R. P. H. KOOYMAN, G. H. M. ENGBERS and J. FEIJEN, *Biomaterials* **18** (1997) 845.
30. A. J. KUIJPERS, P. B. WACHEM, M. J. A. LUYN, L. A. BROUWER, G. H. M. ENGBERS, J. KRIJGSVELD, S. A. J. ZAAT, J. DANKERT and J. FEIJEN, *ibid.* **21** (2000) 1763.
31. M. LESTELIUS, B. LIEDBERG and P. TENGVALL, *Langmuir* **13** (1997) 5900.
32. A. R. NOBLE-LUGINBUHI and R. G. NUZZO, *ibid.* **17** (2001) 3937.
33. C. E. D. CHIDSEY and D. N. LOIACONO, *ibid.* **6** (1990) 682.
34. P. E. LAIBINIS, G. M. WHITESIDES, D. L. ALLARA, Y. T. TAO, A. N. PARIKH and R. G. NUZZO, *J. Am. Chem. Soc.* **113** (1991) 7152.
35. Y. ITO, M. KAJIHARA and Y. IMANISHI, *J. Biomed. Mater. Res.* **25** (1991) 1325.
36. Y. C. TYAN, J. D. LIAO, S. P. LIN and C. C. CHEN, *ibid.* **67A** (2003) 1033.
37. J. F. MOULDER, W. F. STICKLE, P. E. SOBOL and K. D. BOMBEN, in "Handbook of X-ray Photoelectron Spectroscopy" (Physical Electronics, Inc. Minnesota, 1995).
38. G. BEAMSON and D. BRIGGS, in "High Resolution XPS of Organic Polymers. The Scienta ESCA300 Database" (Wiley & Sons Inc., New York, 1992).

Received 20 February
and accepted 19 July 2004